A simple triangular multilayer Kirchhoff-Love shell element

Gustavo C. Gomes[1], Paulo M. Pimenta[1], Adnan Ibrahimbegovic[2]

[1]*Polythechnic School at University of São Paulo*
Av. Prof. Almeida Prado, trav. 2 n° 83 Edifício Paula Souza, 05424-970, São Paulo, Brazil
gustavocanario@usp.br, ppimenta@usp.br
[2] *Université de Technologie de Compiègne*
Alliance Sorbonne Universités, Laboratoire de Mécanique, Compiègne, France
adnan.ibrahimbegovic@utc.fr

Abstract. This paper presents a new triangular multi-layer nonlinear shell finite element suitable for simulation with large displacements and rotations. This is a nonconforming element with 6 nodes, a quadratic displacement and a linear rotation field based on Rodrigues incremental rotation parameters, having in total 21 degrees of freedom. The novelty of this element concerns the extension to a multilayer situation of the T6-3iKL element, a kinematical model with properties from Kirchhoff-Love theory, approximating the shell director across the layers as constant and the rotation-continuity between adjacent elements, allowing multiple branches connections in the mesh. These kinematical assumptions make the element extremely simple, without need of artificial parameters such as penalties. The element allows implementation of different material constitutive equations. The model is numerically implemented and displacement results are compared to different references in multiple examples, showing the consistency and robustness of the formulation. It is believed that the multilayer extension conserving all the desirable properties of the T6-3iKL (such as no necessity of penalty, simple kinematic, a relatively small number of DoFs, geometric exact, possibility to use 3D material models, easily connected with multiple branched shells and beams) and including possibly the simplest multilayer model, create a simple yet powerful shell element.

Keywords: Triangular Shell Element, Multilayer shell, Nonlinear Shell Formulation, Kirchhoff-Love shell, Large Strains.

1 Introduction

In this work we present an extension of the triangular Kirchhoff-Love shell element T6-i3KL developed in [1] to the multi-layer consideration, creating a new element.

The main multi-layer consideration used to build the element is based on the thin nature of Kirchhoff-Love shells. It is assumed that rotation along the layers remains constant, regardless of possible change of material and thickness. This consideration greatly simplifies the multi-layer kinematics and eliminate the need of multiple independent variables along the thickness. The theory defines the energy of the system by conjugating the first Piola-Kirchhoff stress tensor and the deformation gradient, allowing for contribution of each layer in the internal energy of the shell.

We assume a plane reference configuration for the mid-surface, and the rotation is considered with the Rodrigues formula, in a pure lagrangian way, considering Rodrigues parameter and incremental rotation. In the present work, we have a nonconforming element with 6 nodes, a quadratic displacement and a linear rotation field based on Rodrigues incremental rotation parameters, giving in total 21 degrees of freedom. The numerical implementation is done using AceGen and AceFEM, fully utilizing the automation of the packages as a mean to obtain physical quantities such as the residual force vector and the stiffness matrix.

In regard to the notation considered throughout the text, italic Latin or Greek lowercase letters (a, b, ..., α, β) denote scalars quantities, bold italic Latin or Greek lowercase letters ($\mathbf{a}, \mathbf{b}, \ldots, \boldsymbol{\alpha}, \boldsymbol{\beta}$) denote vectors, bold italic Latin or Greek capital letters ($\mathbf{A}, \mathbf{B}, \ldots$) denote matrix and second order tensors. Summation convention over repeated indices, with values $\{1, 2, 3\}$ for latin letters and $\{1, 2\}$ for greek letters

2 Shell formulation

2.1 Multi—Layer consideration

The main consideration that guides the current multi-layer theory is that, due to the thin nature of the Kirchhoff-Love shell, the consideration that the shell director does not change direction along each layer, see Fig. 1. This greatly simplifies the multi-layer kinematics, as there is no need of specific inter-layer displacement equations to deal with the shell director variation along the thickness, as usually is the case for Reissner-Mindlin models.

In the model, we assume the middle plane of the shell as the reference to obtain the kinematics equations and to apply the FEM mesh and external loads.

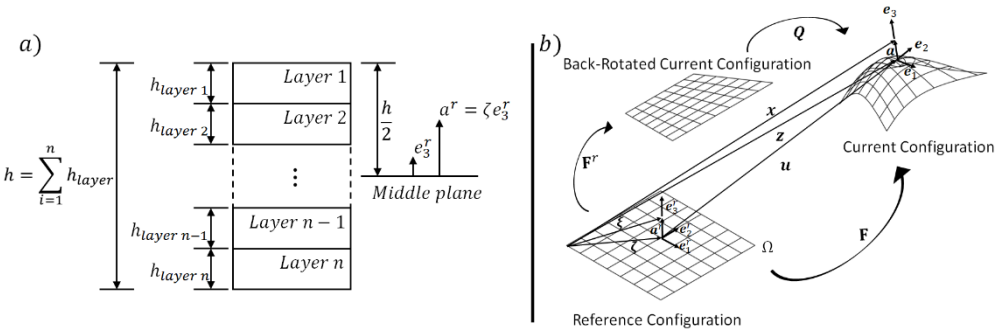

Figure 1 – a) Shell director along layers; b) Shell description and kinematics

2.2 Kinematics

It is assumed that the middle plane is in the reference configuration of the shell and it is flat, see Fig. 1, with an orthogonal coordinate system $\{\boldsymbol{e}_1^r, \boldsymbol{e}_2^r, \boldsymbol{e}_3^r\}$ where $\boldsymbol{e}_1^r$ and $\boldsymbol{e}_2^r$ are in the middle plane of the shell and $\boldsymbol{e}_3^r$ is normal to the plane. In the current configuration, the orthogonal coordinate system is $\{\boldsymbol{e}_1, \boldsymbol{e}_2, \boldsymbol{e}_3\}$, with the relation $\boldsymbol{e}_i = \boldsymbol{Q}\boldsymbol{e}_i^r$ valid, where $\boldsymbol{Q}$ is the rotation tensor.

The definition of any point in the reference configuration will then be given by

$$\boldsymbol{\xi} = \boldsymbol{\zeta} + \boldsymbol{a}^r, \boldsymbol{\zeta} = \xi_\alpha \boldsymbol{e}_\alpha^r \in \Omega^r \text{ and } \boldsymbol{a}^r = \zeta \boldsymbol{e}_3^r \in H^r, \tag{1}$$

where $\boldsymbol{\zeta}$ are the coordinates of a material point in the shell middle plane and $\boldsymbol{a}^r$ is the fiber direction of the shell at this point. The thickness h of the shell in the reference configuration is considered through the parameter $\zeta \in \mathrm{H} = [-h^b, h^t]$, where $h = h^b + h^t$.

Similarly to the definition of a material point in the reference configuration, the definition of any point in the current is given by

$$\boldsymbol{x} = \boldsymbol{z} + \boldsymbol{a}, \boldsymbol{z} = \boldsymbol{\zeta} + \boldsymbol{u} \text{ and } \boldsymbol{a} = \boldsymbol{Q}\boldsymbol{a}^r, \tag{2}$$

$\boldsymbol{z}$ represents the current position of a point in the middle surface and $\boldsymbol{a}$ the position along the thickness of the shell, in $\boldsymbol{e}_3$ direction.

Adopting the notation $\partial(\cdot)/\partial(\xi_\alpha) = (\cdot)_{,\alpha}$, the deformation gradient can be obtained from:

$$\mathbf{F} = \boldsymbol{x}_{,\alpha} \otimes \boldsymbol{e}_\alpha^r + \frac{\partial \boldsymbol{x}}{\partial \zeta} \otimes \boldsymbol{e}_3^r = \boldsymbol{f}_a \otimes \boldsymbol{e}_\alpha^r + \boldsymbol{f}_3 \otimes \boldsymbol{e}_3^r = \left(\boldsymbol{z}_{,\alpha} + \boldsymbol{\kappa}_\alpha \times \boldsymbol{a}\right) \otimes \boldsymbol{e}_\alpha^r + \boldsymbol{Q}\boldsymbol{e}_3^r \otimes \boldsymbol{e}_3^r. \tag{3}$$

where

$$\boldsymbol{K}_\alpha = \boldsymbol{Q}_{,\alpha}\boldsymbol{Q}^{\mathrm{T}} \text{ and } \boldsymbol{\kappa}_\alpha = axial(\boldsymbol{K}_\alpha). \tag{4}$$

The back-rotated counterparts of the deformation gradient and the strains is defined as

$$\boldsymbol{F}^r = \boldsymbol{Q}^{\mathrm{T}}\boldsymbol{F} = \boldsymbol{I} + \boldsymbol{\gamma}_\alpha^r \otimes \boldsymbol{e}_\alpha^r, \tag{5}$$

with

$$\boldsymbol{\gamma}_\alpha^r = \boldsymbol{\eta}_\alpha^r + \boldsymbol{\kappa}_\alpha^r \times \boldsymbol{a}^r\,; \qquad \boldsymbol{\eta}_\alpha^r = \boldsymbol{Q}^T \boldsymbol{z}_{,\alpha} - \boldsymbol{e}_\alpha^r; \qquad \boldsymbol{\kappa}_\alpha^r = \text{axial}\big(\boldsymbol{Q}^{\mathrm{T}} \boldsymbol{Q}_{,\alpha}\big) = \boldsymbol{Q}^{\mathrm{T}} \boldsymbol{\Gamma}_\beta \boldsymbol{u}_{,\beta\boldsymbol{\alpha}} \tag{6}$$

It is important to remark that, due to the Kirchhoff-Love assumption, $\boldsymbol{\gamma}_\alpha^r \cdot \boldsymbol{e}_3^r = \boldsymbol{\eta}_\alpha^r \cdot \boldsymbol{e}_3^r = 0$.

2.3 Variational formulation and material equations

The stiffness matrix of the current work is obtained through the variational formulation and with the help of AceGen. The usage of this software allows for a plethora of material models readily implemented with automatic differentiation, as long as the material model is given with a strain energy function. In order to assure the convergence of the simulations, we work here with two polyconvex material models suitable for large displacements and rotations.

As the materials considered are hyperelastic, there exists a total strain energy function ψ that describes the elastic energy stored in the body. Here, we define the functional

$$\prod(\boldsymbol{u}) = \int_B \big(\psi(\boldsymbol{C}(\boldsymbol{u})) - \rho_0 \bar{\boldsymbol{b}} \cdot \boldsymbol{u}\big) dV - \int_{\partial B} (\bar{\boldsymbol{t}} \cdot \boldsymbol{u}) dA. \tag{7}$$

The directional derivative of the functional is obtained as

$$\delta \prod(\boldsymbol{u}) = D \prod(\boldsymbol{u}) \cdot \boldsymbol{v} = \frac{\partial}{\partial \alpha} \prod(\boldsymbol{u} + \alpha \boldsymbol{v})_{\alpha=0} = 0. \tag{8}$$

One can define the internal total energy for the shell as

$$\prod(\boldsymbol{u}) = U^{int} = \int_\Omega \int_{H^r} \psi(\xi_1^r, \xi_2^r) dH d\Omega = \int_\Omega \hat{\psi}(\xi_1^r, \xi_2^r) d\Omega. \tag{9}$$

The strain energy is, obviously, material dependent, with two options presented in the current work. The internal stress and material tangent moduli are obtained by

$$\boldsymbol{P} = \frac{\partial \psi}{\partial \boldsymbol{F}} \qquad \text{and} \qquad \boldsymbol{D}_{\alpha\beta}^r = \frac{\partial \boldsymbol{\sigma}_\alpha^r}{\partial \boldsymbol{\varepsilon}_\alpha^r} = \frac{\partial^2 \bar{\psi}}{\partial \boldsymbol{\varepsilon}_\alpha^r \partial \boldsymbol{\varepsilon}_\beta^r}. \tag{10}$$

The first material described is the Ciarlet-Simo Neo-Hookean isotropic material, defined by the polyconvex strain energy function

$$\psi = \frac{1}{2}\lambda\left(\frac{1}{2}(J^2 - 1) - \ln(J)\right) + \frac{1}{2}\mu(I_1 - 3 - 2\ln(J)), \tag{11}$$

with the invariants, Cauchy-Green stress tensor and Lamé coefficients given as

$$I_1 = tr\,\boldsymbol{C} = \boldsymbol{f}_i \cdot \boldsymbol{f}_i, \quad I_2 = \boldsymbol{tr}(\text{Cof}\,\boldsymbol{C}) = \boldsymbol{g}_i \cdot \boldsymbol{g}_i \quad \text{and} \quad I_3 = \det \boldsymbol{C} = J^2 = \big(\boldsymbol{f}_1 \cdot (\boldsymbol{f}_2 \times \boldsymbol{f}_3)\big)^2, \tag{12}$$

$$\boldsymbol{C} = \boldsymbol{F}^{\mathrm{T}} \boldsymbol{F}, \tag{13}$$

$$\lambda = \frac{E\nu}{(1+\nu)(1-2\nu)} \qquad \text{and} \qquad \mu = \frac{E}{2(1+\nu)}. \tag{14}$$

The second material is anisotropic, polyconvex in both the isotropic and anisotropic contributions, as presented in [1], [2] and [3] and is given as

$$\psi(\boldsymbol{C}) = \psi^{i\_p}(\boldsymbol{C}) + \psi^{a\_p}(\boldsymbol{C}) = \psi^{i\_p}(\boldsymbol{C}) + \sum_i^2 \alpha_1^{(i)} \langle I_4^{(i)} - 1 \rangle^{\alpha_2^{(i)}}, \tag{15}$$

where $\alpha_1^{(i)}$ and $\alpha_2^{(i)}$ are variables in relation to material properties in the $\boldsymbol{m}^{(i)}$ direction, "$\langle \quad \rangle$" are Macaulay brackets and $I_4^{(i)}$ and $I_5^{(i)}$ are invariants defined as

$$I_4^{(i)} = tr\big[A_{\alpha\beta}^{(i)} \boldsymbol{f}_\alpha \cdot \boldsymbol{f}_\beta\big] \qquad \text{and} \qquad I_5^{(i)} = A_{\alpha\beta}^{(i)} \boldsymbol{g}_\alpha \cdot \boldsymbol{g}_\beta, \tag{16}$$

with

$$A_{\alpha\beta}^{(i)} = \big(\boldsymbol{e}_\alpha \cdot \boldsymbol{m}^{(i)}\big)\big(\boldsymbol{e}_\beta \cdot \boldsymbol{m}^{(i)}\big) = \boldsymbol{e}_\alpha \cdot \boldsymbol{M}^{(i)} \boldsymbol{e}_\beta \qquad \text{and} \qquad \boldsymbol{M}^{(i)} = \boldsymbol{m}^{(i)} \otimes \boldsymbol{m}^{(i)}. \tag{17}$$

In relation to the isotropic part, we use the neo-Hookean material model previously presented.

2.4 Plane stress

The plane stress condition is a necessity when the shell theory does not consider thickness variation. As such, the present work enforces this condition analytically for the presented materials by adding the term $\boldsymbol{\gamma}_{33}^r = \gamma_{33}\boldsymbol{e}_3^r$ to eq. (5), rewriting it as

$$\boldsymbol{F}^r = \boldsymbol{I} + \boldsymbol{\gamma}_\alpha^r \otimes \boldsymbol{e}_\alpha^r + \boldsymbol{\gamma}_{33}^r \otimes \boldsymbol{e}_3^r. \tag{18}$$

The plane stress is then enforced by $\tau_{33} = \boldsymbol{\tau}_3^r \cdot \boldsymbol{e}_3^r = 0$.

With eq. (10), eq. (11) and eq. (18), one arrives at

$$\tau_{33} = 2(1+\gamma_{33})\frac{\partial \psi}{\partial I_1} + \frac{\partial \psi}{\partial J}\bar{J}, \tag{19}$$

where $\bar{J} = \boldsymbol{e}_3^r \cdot (f_1^r \times f_2^r)$. After some manipulations, one arrives at

$$\gamma_{33} = \sqrt{\frac{\lambda + 2\mu}{\lambda \bar{J}^2 + 2\mu}} - 1. \tag{20}$$

3 Rotation Field

3.1 Rodrigues rotation vector

The rotation vector can be represented as $\boldsymbol{\theta} = \theta \boldsymbol{e}$, with θ being the rotation around the axis $\boldsymbol{e}$. As presented in [4], the rotation tensor can be a function of the Rodrigues rotation vector as $\boldsymbol{\alpha} = \frac{\boldsymbol{tan}(\theta/2)}{\theta/2}\boldsymbol{\theta}$, restricting the rotation at $-\pi < \theta < +\pi$. As such, the rotation tensor can be defined as

$$\boldsymbol{Q} = \boldsymbol{I} + h(\alpha)\left(\boldsymbol{A} + \frac{1}{2}\boldsymbol{A}^2\right), \quad \text{with} \quad h(\alpha) = \frac{4}{4+\alpha^2}, \tag{21}$$

$\alpha = \|\boldsymbol{\alpha}\|$ and $\boldsymbol{A} = \boldsymbol{Skew}(\boldsymbol{\alpha})$.

3.2 Incremental description of rotation

The incremental rotational variables are presented as

$$\boldsymbol{Q}_\Delta = \boldsymbol{I} + h(\alpha_\Delta)\left(\boldsymbol{A}_\Delta + \frac{1}{2}\boldsymbol{A}_\Delta^2\right), \quad \text{with} \quad h(\alpha_\Delta) = \frac{4}{4+\alpha_\Delta^2}, \tag{22}$$

where $\alpha_\Delta = \|\boldsymbol{\alpha}_\Delta\|$ and $\boldsymbol{A}_\Delta = Skew(\boldsymbol{\alpha}_\Delta)$.

The update of the rotation tensor is done by

$$\alpha_{i+1} = \frac{4}{4 - \boldsymbol{\alpha}_i \cdot \boldsymbol{\alpha}_\Delta}\left(\boldsymbol{\alpha}_i + \boldsymbol{\alpha}_\Delta - \frac{1}{2}\boldsymbol{\alpha}_i \times \boldsymbol{\alpha}_\Delta\right), \tag{23}$$

where $\boldsymbol{\alpha}_{i+1}$ is the next step of $\boldsymbol{\alpha}_i$. We also update the rotation tensor following the relations

$$\boldsymbol{Q}_{i+1} = \boldsymbol{Q}_\Delta \boldsymbol{Q}_i, \text{ with } \boldsymbol{Q}_{i+1} = \hat{Q}(\boldsymbol{\alpha}_{i+1}), \quad \boldsymbol{Q}_\Delta = \hat{Q}(\boldsymbol{\alpha}_\Delta) \quad \text{and} \quad \boldsymbol{Q}_i = \hat{Q}(\boldsymbol{\alpha}_i). \tag{24}$$

As $\boldsymbol{Q}$ applies to the shell director, one may also define

$$\boldsymbol{e}_3^{i+1} = \boldsymbol{Q}_\Delta \boldsymbol{e}_3^i. \tag{25}$$

Here we bring the description of the rotation vector in relation to a scalar parameter φ_Δ, first presented in [5] in relation to vector $\boldsymbol{e}_3$ and, here, described in relation to $\boldsymbol{e}_1$ to obtain the rotation vector in agreement with [6]. This is done as $\boldsymbol{e}_1$ can be calculated only by displacement. As so, we have

$$\boldsymbol{\alpha}_\Delta = \frac{\boldsymbol{e}_1^i \times \boldsymbol{e}_1^{i+1}}{\|\boldsymbol{e}_1^m\|^2} + \varphi_\Delta \frac{\boldsymbol{e}_1^m}{\|\boldsymbol{e}_1^m\|}, \quad \text{with} \quad \boldsymbol{e}_1^m = \frac{1}{2}\left(\boldsymbol{e}_1^{i+1} + \boldsymbol{e}_1^i\right). \tag{26}$$

The curvature vectors presented in eq. (4) and eq. (6) can be rewritten in relation to Rodrigues rotation parameters as

$$\boldsymbol{\kappa}_\alpha^r = \boldsymbol{\Xi}^{\mathrm{T}} \boldsymbol{\alpha}_{,\alpha} \quad \text{and} \quad \boldsymbol{\kappa}_\alpha = \boldsymbol{\Xi} \boldsymbol{\alpha}_{,\alpha} \quad \text{with} \quad \boldsymbol{\Xi} = \frac{4}{4+\boldsymbol{\alpha}^2}\left(\boldsymbol{I} + \frac{1}{2}\boldsymbol{A}\right). \tag{27}$$

In the same fashion as in [7], we use the incremental formulation of the curvature vectors as

$$\boldsymbol{\kappa}_{i+1}^r = \boldsymbol{\kappa}_{\alpha i}^r + \Delta\boldsymbol{\kappa}_\alpha^r, \text{ with } \Delta\boldsymbol{\kappa}_\alpha^r = \det(\boldsymbol{Q}_{1/2})\boldsymbol{Q}_{1/2}^{-1}\boldsymbol{\alpha}_{\Delta,\alpha}, \text{ and } \boldsymbol{Q}_{1/2} = \left(\boldsymbol{I} + \frac{1}{2}\boldsymbol{A}_\Delta\right)^{-1}\boldsymbol{Q}_{i+1}. \tag{28}$$

Regarding the rotation, it is implemented incrementally and as so, at every step the rotation vector $\boldsymbol{\alpha}$ is updated as

$$\boldsymbol{\alpha}_{i+1} = \frac{4}{4 - \boldsymbol{\alpha}_i \cdot \boldsymbol{\alpha}_\Delta}\left(\boldsymbol{\alpha}_i + \boldsymbol{\alpha}_\Delta - \frac{1}{2}\boldsymbol{\alpha}_i \times \boldsymbol{\alpha}_\Delta\right), \tag{29}$$

with $\boldsymbol{\alpha}_\Delta$ updated as in eq. (26). Regarding the curvature vector, it is incremented as in eq. (28).

At every step, the increment parameters are reset as $\boldsymbol{\alpha}_\Delta = \boldsymbol{0}$, $\varphi_\Delta = 0$, and $\Delta\boldsymbol{\kappa}_\alpha^r = \boldsymbol{0}$.

4 The Finite Element

The element used is an extrapolation of the T6-3iKL seen in [6], a six-noded displacement based triangular element (see Fig. 2). The discretization of the element coordinates and displacement field is done with area coordinates and quadratic interpolation and, an additional scalar rotation parameter (φ_Δ). The rotation vector $\boldsymbol{\alpha}$ is a linear non-conform field over the shell element obtained indirectly by the scalar DoF φ_Δ shared between adjacent elements. This model renders a quite efficient element, with a reduced number of DoF when compared with usual models that consider the rotation using three-dimensional vectors as DoF. This characteristic associated with the simplification of the continuous shell director along the multi-layers, constitutes an incredibly simple and efficient multi-layer element.

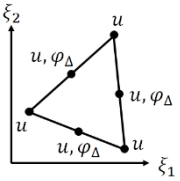

Figure 2 – T6-i3KL

This recent description of the rotation, proposed in [6] is a quite interesting adoption, reducing the number of DoF involved in the analysis while not reducing the quality of results. Such advantage is fully used in the present work with the adoption of a constant rotation through the layers of the element due to the small thickness.

The element uses 3 integration points at the mid-side nodes of the shell plane and, when integrating along the thickness, each layer has 3 integration points, using Simpson's 1/3 rule. Obviously, by integrating each layer separately, one allows for use of different materials and thickness at each layer.

5 Results

5.1 Cantilever Beam

The cantilever beam was an example proposed in [8], revisited in [9], [10] and [6] to analyze the behavior of the element when used under conditions of high rotations and displacement in and out of plane, in this work, with multiple layers possibility. As for the geometry and the mesh, shown in Fig. 3, a cross section of $b = 0.1 \times h =$

0.1 is used, with length $L = 1.0$. One end of the beam is clamped, while the other is subjected to different values of a concentrated force P, variable from 0 to 1000. The beam material has an Young's modulus $E = 10^7$ and poisson's ratio $v = 0.3$ for all the layers, with Neo-Hookean material model.

The values for comparison are the results of displacement of the midpoint of the free end of the beam, which are compared with that obtained in the work of [9], where the maximum deflection are $u_{in-plane} = 0.8425$ and $u_{out-of-plane} = 0.8406$.

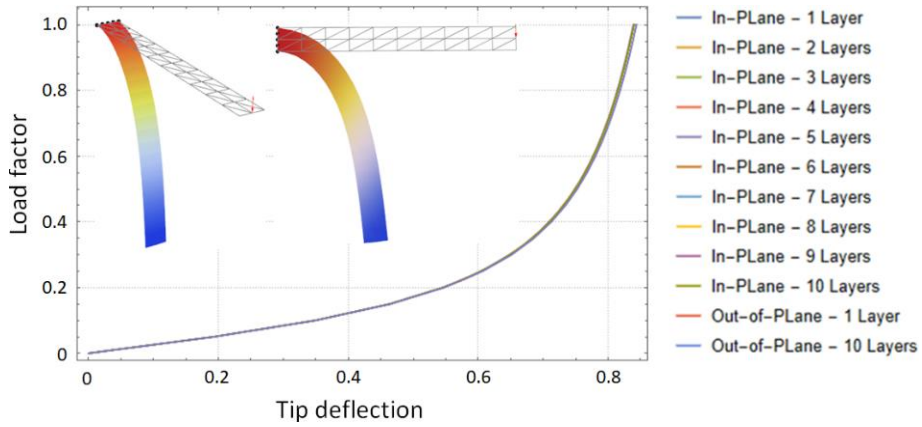

Figure 3 – In and out of plane cantilever beam

5.2 Pinched cylinder

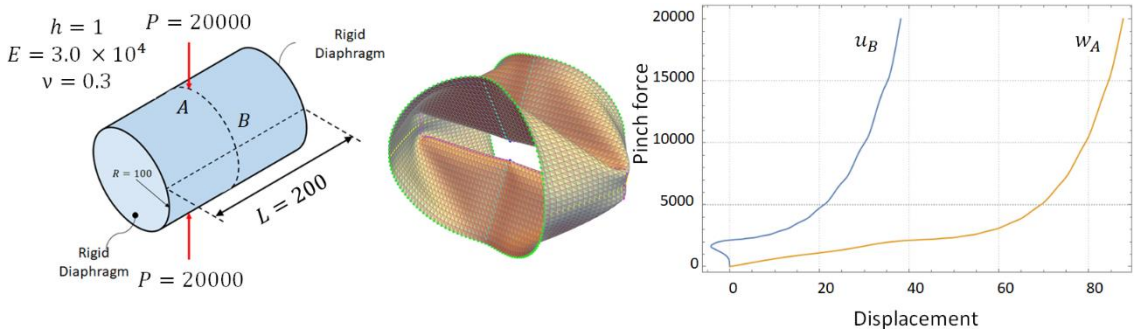

Figure 4 – Pinched cylinder

This is another classic in the literature, referring to [6] for results comparison. The cylinder has a radius of $R = 100$, length of $L = 200$ and thickness $h = 1$. The material used is Neo-hookean for all the 3 layers, with Young's modulus $E = 3 \cdot 10^4$ and poisson's coefficient $v = 0.3$. The pinch force applied symmetrically at top and bottom is $P = 20000$.The mesh and results for displacement of points A and B, are presented in Fig. 4.

5.3 Wrinkling of membrane

This example is used to verify the anisotropic capability of the shell multi-layered element. The square membrane has side equal to 1 and beveled corners to avoid stress concentration. The vertical corners are clamped, and the horizontal corners are stretched by a distributed force $q = 0.1$. To ensure the wrinkling behaviour, some of the points in the mesh are moved, in order to remove symmetry and allow the beginning of wrinkling. The material used is the anisotropic model presented in a previous section, with orthotropic direction $m_1 = [0,1,0]^{\mathrm{T}}$ and $m_2 = [1,0,0]^{\mathrm{T}}$. The isotropic parameters for the Neo-Hookean analysis are $E = 200$ and $v = 0.3$. The anisotropic parameters are $\alpha_1 = 4$ and $\alpha_2 = 2.3$ for the warp direction and $\alpha_1 = 1$ and $\alpha_2 = 2.3$ for the weft direction. For comparison, we refer to [6]. The example was modeled with 1 to 9 layers and the results for deformation and the dimensions are presented in Fig. 5.

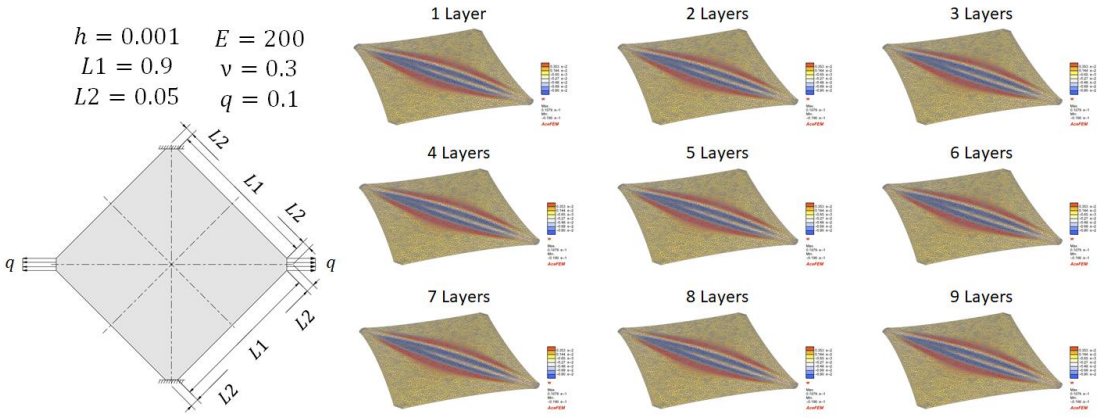

Figure 5 – Wrinkling of a membrane

6 Conclusions

As seen in the current work, the context of a thin shell with Kirchhoff-Love theory and consequent assumption of a constant direction of the shell director connected with a multi-layer approach, create an extremely simple multi-layer finite element. The results from the numerical implementation indicate that, although simple, the element performed exceedingly well for the examples here presented and many others omitted due to length constraints. For the next step with the current theory, the authors intend to focus on stress analysis along the layers.

Acknowledgements. Gustavo C. Gomes acknowledges the financial support by CNPq and all the authors thankfully acknowledges FAPESP (contract/grant number: 2020/13362-1).

Authorship statement. The authors hereby confirm that they are the sole liable persons responsible for the authorship of this work, and that all material that has been herein included as part of the present paper is either the property (and authorship) of the authors, or has the permission of the owners to be included here.

References

[1] Sanchez M. L., Pimenta P. M., Ibrahimbegovic A., A Simple Geometrically Exact Shell Finite Element. Part 1: Statics. *Computer Methods in Applied Mechanics and Engineering*, 2022.

[2] Viebahn N., Pimenta P. M., Schröder J., A simple triangular finite element for nonlinear thin shells: statics, dynamics and anisotropy. *Computational Mechanics*, p. 281-297, 2017.

[3] Schröder J., Neff P., Poly-, quasi-and rank-one convexity in applied mechanics. *Springer Science & Business*, 2010.

[4] Schröder J., Viebahn N., Balzani D., Wriggers P., A novel mixed finite element for finite anisotropic elasticity: the SKA-element. *cmiamae*, p. 475-494, 2016.

[5] Campello E. M. B., Pimenta P. M., Wriggers P., A triangular finite shell element based on a fully nonlinear shell formulation. *Computational Mechanics*, v. 31, p. 505-518, 2003.

[6] Silva C., Maassen S., Pimenta P. M., Schröder J., A simple finite element for the geometrically exact analysis of bernoulli–euler rods. *Computational Mechanics*, p. 1-19, 2019.

[7] Campello E. M. B., Pimenta P. M., Wriggers P., An exact conserving algorithm for nonlinear dynamics with rotational dofs and general hyperelasticity. part 2: shells. *Computational Mechanics*, p. 195-211, 2011.

[8] Simo J. C., Fox D. D., Rifai M. S., On a stress resultant geometrically exact shell model. Part III: computational aspects of the nonlinear theory. *Comp. Meth. Appl. Mech. Engrg.*, p. 21-70, 1990.

[9] Wriggers P., Gruttmann F., Thin shells with finite rotations formulated in Biot stresses: theory and finite element formultation. *Int. J. Numer. Meth. Engrg.*, p. 2049-2071, 1993.

[10] Campello E. M. B., Pimenta P. M., Wriggers P., A triangular finite shell element based on a fully nonlinear shell formulation. *Computational Mechanics*, v. 31, p. 505-518, 2003.